

Structural and dielectric studies of $\text{BaFe}_{0.5}\text{Nb}_{0.5}\text{O}_3$

This article has been downloaded from IOPscience. Please scroll down to see the full text article.

2002 J. Phys.: Condens. Matter 14 249

(<http://iopscience.iop.org/0953-8984/14/2/311>)

View [the table of contents for this issue](#), or go to the [journal homepage](#) for more

Download details:

IP Address: 171.66.16.238

The article was downloaded on 17/05/2010 at 04:44

Please note that [terms and conditions apply](#).

Structural and dielectric studies of $\text{BaFe}_{0.5}\text{Nb}_{0.5}\text{O}_3$

Sonali Saha and T P Sinha

Department of Physics, Bose Institute, 93/1, Acharya Prafulla Chandra Road, Kolkata-700009, India

Received 4 September 2001, in final form 13 November 2001

Published 13 December 2001

Online at stacks.iop.org/JPhysCM/14/249

Abstract

Ferroelectric $\text{BaFe}_{0.5}\text{Nb}_{0.5}\text{O}_3$ (BFN) ceramic is synthesized by the solid-state reaction technique for the first time. The x-ray diffraction of the sample at room temperature shows a monoclinic phase. Dielectric studies of the sample show a frequency dependence of the temperatures at which the dielectric permittivity (real and imaginary) peaks. The temperature variations of the real and imaginary components of the dielectric permittivity show broad maxima. There is evidence for Vogel–Fulcher-type relaxational freezing. The analysis of the real and imaginary parts of the dielectric permittivity with frequency has been performed assuming a distribution of relaxation times as confirmed by Cole–Cole plots as well as the scaling behaviour of the dielectric loss. All these observations clearly suggest that BFN is a relaxor ferroelectric. The Mössbauer spectrum of the sample at room temperature shows a symmetric doublet, with the iron being trivalent.

1. Introduction

In recent years there has been a considerable amount of interest in the investigation of relaxor ferroelectrics, i.e., the ferroelectrics having a diffuse phase transition (DPT) which is characterized by a broad maximum in the temperature dependence of the dielectric permittivity ϵ' (real part) and the dielectric dispersion in the transition region (Smolensky 1970, 1984). Lead magnesium niobate, $\text{PbMg}_{1/3}\text{Nb}_{2/3}\text{O}_3$ (PMN), can be considered a model system for such investigations of the 1:2 family (Christen *et al* (1994), Vakhrushev *et al* (1994), Colla *et al* (1992), Viehland *et al* (1990), (1991) and references therein) while lead iron niobate, $\text{PbFe}_{0.5}\text{Nb}_{0.5}\text{O}_3$ (PFN), is known to be the most intensively investigated system of 1:1 type (Ivanov *et al* (2000), Lampis *et al* (1999), Darlington (1991), Yasuda and Ueda (1989a, 1989b) and references therein). PFN is a ferroelectric of the disordered type (Smolensky *et al* 1958, Bokov *et al* 1962) having a ferroelectric transition temperature at 110 °C (Bhat *et al* 1974, Brunskill *et al* 1981). It is currently of interest as a component in commercial electroceramic materials, particularly as it is typically characterized by high relative permittivities and low sintering temperatures. Although the structural, dielectric and many other properties of PFN (Ivanov *et al* (2000), Lampis *et al* (1999), Bonny *et al* (1997), Schmid (1994), Bokov *et al*

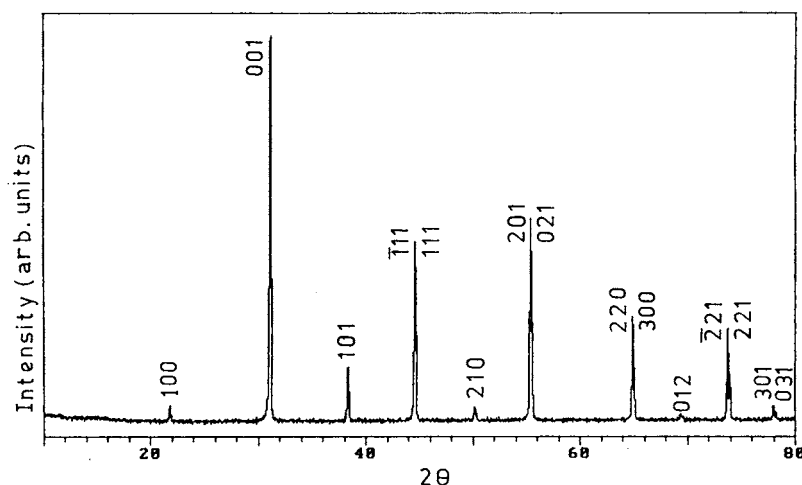


Figure 1. The XRD pattern of BFN at room temperature.

(1993), Yokosuka (1993), Lemanov *et al* (1992), Rayevsky *et al* (1992), Darlington (1991), Yasuda and Ueda (1989a, 1989b), Mabud (1984) and references therein) have been extensively examined, no attempt has been made to study the similar system $\text{BaFe}_{0.5}\text{Nb}_{0.5}\text{O}_3$ (BFN) to our knowledge. In the present work, a dielectric study of BFN ceramic prepared by the solid-state reaction technique is presented for the first time.

2. Experiments

BFN ceramic was prepared using the solid-state reaction technique. Powders of BaCO_3 (reagent grade), Fe_2O_3 of purity 99.99% and Nb_2O_5 (reagent grade) were taken in the stoichiometric ratio and mixed in the presence of acetone for a day. The mixture was calcined in a Pt crucible at 1200°C in air for 10 h and brought to room temperature under controlled cooling. The calcined sample was pelletized into a disc using polyvinyl alcohol as the binder. Finally, the discs were sintered at 1250°C for 5 h and cooled down to room temperature by adjusting the cooling rate.

X-ray powder diffraction pattern of the sample was taken at room temperature using Philips PW1877 automatic x-ray powder diffractometer. For the dielectric characterization, the sintered disc (of thickness 0.72 mm and diameter 12 mm) was polished, gold sputtered and then soldered with silver paste to the LCR meter electrodes. The sample was found to have low resistivity (of the order of $10^8 \Omega \text{ cm}$ at room temperature). The dielectric permittivity of the sample was measured from 10 Hz to 2 MHz in the temperature range from -100 to 200°C . The temperature was controlled with a self-design programmable oven. All the dielectric data were collected while heating at a rate of $0.5^\circ\text{C min}^{-1}$. These results were found to be reproducible.

The Mössbauer absorption experiment was carried out for BFN at room temperature with a constant-acceleration spectrometer which utilized a rhodium matrix ^{57}Co source and was calibrated with α -iron foil. The thickness of the sample was approximately 10 mg cm^{-2} .

3. Results and discussion

Figure 1 shows the x-ray diffraction pattern of the sample taken at room temperature. All the reflection peaks of the x-ray profiles were indexed and lattice parameters were determined using the least-squares method with the help of a standard computer program (POWD). Good

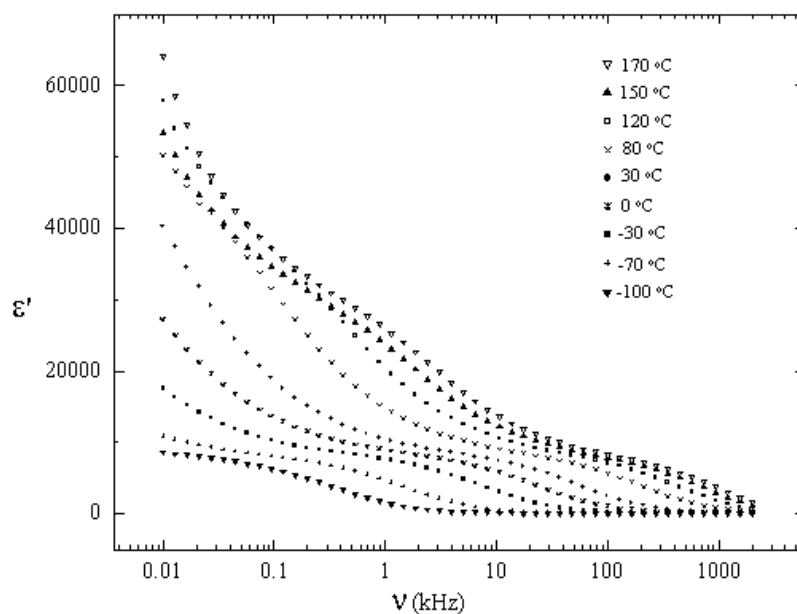


Figure 2. The frequency dependence of ϵ' for BFN at various temperatures.

Table 1. Temperature of the dielectric maximum tabulated alongside the corresponding measurement frequency.

Frequency (kHz)	T'_m (°C)
0.538	172.3
0.690	173.1
0.885	174.7
1.136	176.9
1.457	180.0
1.870	183.2
2.399	187.5

agreement between the observed and calculated interplanar spacing (d -values) suggests that the compound has monoclinic structure at room temperature with $\beta = 90.11^\circ$ ($a = 4.0743 \text{ \AA}$, $b = 4.0388 \text{ \AA}$ and $c = 2.8759 \text{ \AA}$). The x-ray diffraction confirms that the specimen is single phase.

Figure 2 shows the frequency dependence of ϵ' for BFN at various temperatures; these are typical characteristics of ferroelectric material. The temperature dependences of ϵ' at various frequencies in the temperature range from -20 to 200°C are shown in figure 3. It is evident from figure 3 that the variation of ϵ' around T'_m (peak temperature) gets smeared out. These curves demonstrate typical relaxor behaviour with the magnitude of the dielectric permittivity decreasing with increasing frequency and the maximum shifting to higher temperatures. The values of T'_m and the corresponding frequency are tabulated in table 1. Figure 4 shows a plot of $\ln \nu$ versus $1/T'_m$ where the solid circles are the experimental data. It is obvious from figure 4 that the frequency derivative of $1/T'_m$ is smaller at lower frequencies in the observed range. This figure illustrates that as $\nu \rightarrow 0$, a static freezing temperature is approached.

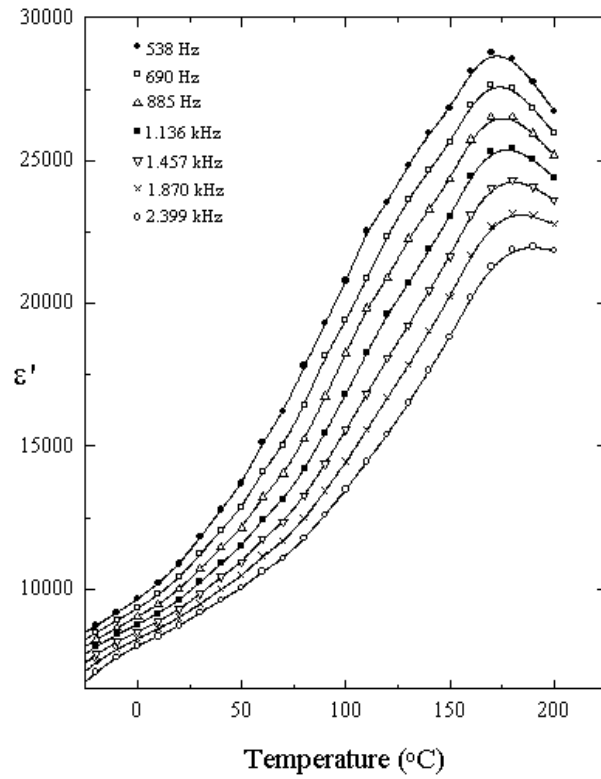


Figure 3. The temperature dependence of ϵ' for BFN at various frequencies.

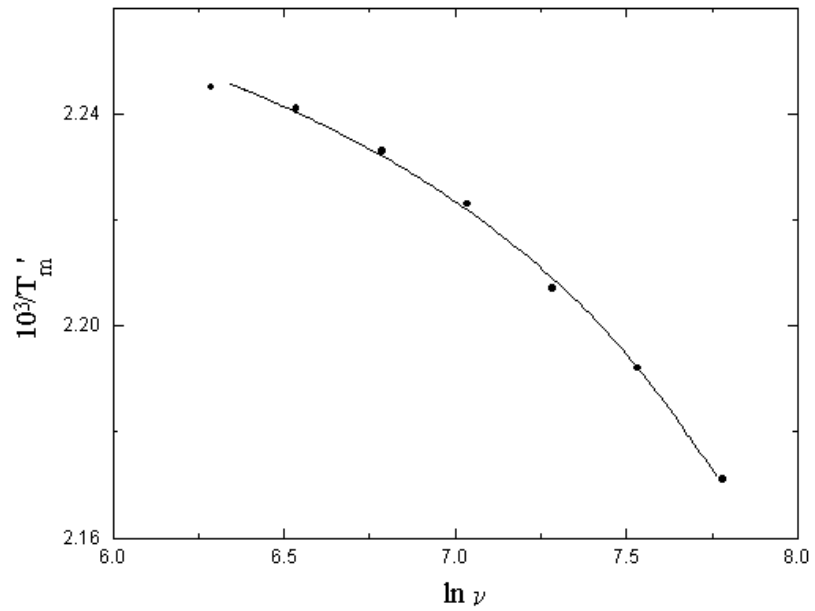


Figure 4. $1/T'_m$ as a function of the measurement frequency of BFN. The solid circles are the experimental points and the solid line is the fit to the Vogel-Fulcher relationship.

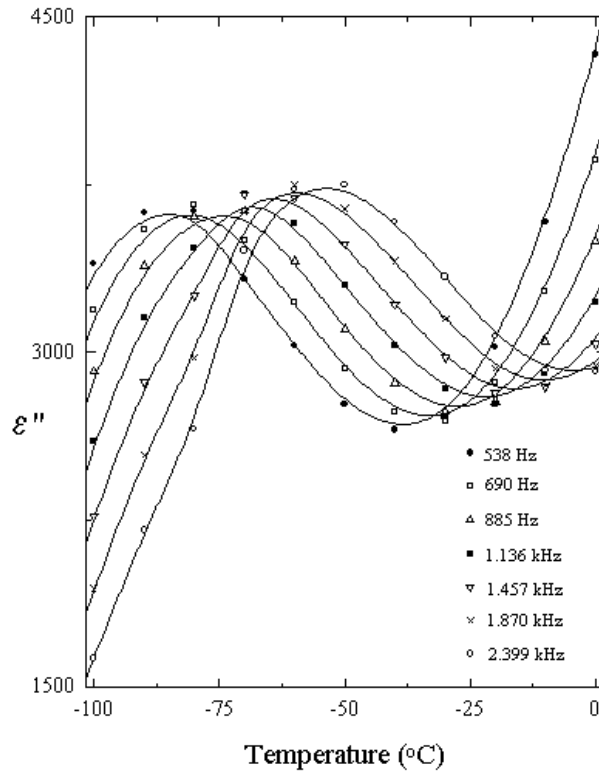


Figure 5. The temperature dependence of ϵ'' for BFN at various frequencies.

The frequency dependence of T'_m can be modelled using the Vogel (1921) and Fulcher (1925) relation given by

$$\nu = \nu_0 \exp \left[\frac{-E_a}{k_B(T'_m - T_f)} \right] \quad (1)$$

where ν_0 is the pre-exponential factor, E_a is the activation energy and T_f is the freezing temperature. In dipolar glass systems, T_f is regarded as the temperature where the dynamic reorientation of dipolar cluster polarization can no longer be thermally activated. The solid line in figure 4 is the curve fitted to the data using equation (1). The values derived from the curve gave an activation energy of 0.004 eV, a pre-exponential factor of 8.2×10^3 Hz and a static freezing temperature of 159 °C. This value of T_f is very reasonable, as it is below the temperature where the maximum occurs. The close agreement of the data with the Vogel–Fulcher relationship suggests that the relaxor behaviour in the BFN is analogous to that of a dipolar glass with polarization fluctuations above a static freezing temperature. The activation energy and pre-exponential factor are both consistent with thermally activated polarization fluctuations.

Figure 5 shows ϵ'' versus temperature plots at various frequencies. The temperature variations in ϵ'' in figure 5 become diffuse and strongly frequency dependent with T''_m (peak temperature) being lower than T'_m , which further supports the suggestion of ferroelectric relaxor behaviour of BFN. It is to be noted that ϵ'' does not peak around T'_m . This behaviour has also been observed in PFN (Yasuda and Ueda 1989a, 1989b).

One of the characteristics of the dipolar glass system as well as relaxor ferroelectrics such as PMN is the appearance (Hochli *et al* 1990, Viehland *et al* 1991, Colla *et al* 1992, Elissalde

et al 1992, Yushin and Dorogovtsev 1993, Christen *et al* 1994) of a low-frequency dielectric loss peak below T'_m in the ϵ'' versus $\log \nu$ plots. Figure 6 shows ϵ'' versus $\log \nu$ plots at various temperatures for BFN. The loss peaks shift to lower frequencies on decreasing the temperature, indicating the thermally activated nature of the dielectric relaxation. These studies have thrown light on the nature of the freezing of dipolar clusters below T'_m . An increase in the value of ϵ'' in the lower-frequency region may be due to the increase in ionic conductivity resulting from the disordering of mobile cations in the oxygen-octahedral skeleton (Beleckas *et al* 1989). It seems clear that the width of the loss peaks in figure 5 cannot be accounted for in terms of a monodispersive relaxation process, and points towards the possibility of a distribution of relaxation times.

One of the most convenient ways for checking the polydispersive nature of dielectric relaxation is through complex Argand plane plots of ϵ'' against ϵ' , usually called Cole–Cole plots (Cole and Cole 1941). For a pure monodispersive Debye process, one expects semicircular plots with the centre located on the ϵ' -axis whereas, for polydispersive relaxation, these Argand plane plots are close to circular arcs with end-points on the axis of reals and the centre below this axis. The complex dielectric constant in such situations is known to be described by the empirical relation

$$\epsilon^* = \epsilon' - i\epsilon'' = \epsilon_\infty + \frac{(\epsilon_s - \epsilon_\infty)}{1 + (i\omega\tau)^{1-\alpha}} \quad (2)$$

where ϵ_s and ϵ_∞ are the low- and high-frequency values of ϵ' , α is a measure of the distribution of relaxation times, $\tau = \omega^{-1}$ and $\omega = 2\pi\nu$. The parameter α can be determined from the location of the centre of the Cole–Cole circles, of which only an arc lies above the ϵ' -axis. Figure 7 depicts two representative plots for $T = -70$ and 100°C . It is evident from these plots that the relaxation process differs from the monodispersive Debye process (for which $\alpha = 0$). The parameter α , as determined from the angle subtended by the radius of the circle with the ϵ' -axis passing through the origin of the ϵ'' -axis, shows a very small increase in the interval $[0.056, 0.078]$ with the decrease of temperature from 100 to -70°C , implying a slight increase in the distribution of the relaxation time with decreasing temperature below T'_m .

The Cole–Cole plots confirm the polydispersive nature of the dielectric relaxation of BFN. However, the small variation in α with decreasing temperature is not convincing enough, keeping in mind the uncertainties in fitting the circle, which was done through a visual fit to the observed data points. We can look at the distribution of relaxation times from yet another angle. If $g(\tau, T)$ is the temperature-dependent distribution function for relaxation times, the complex dielectric constant can be expressed as (Wagner 1913)

$$\epsilon^* - \epsilon_\infty = \epsilon(0, T) \int \frac{g(\tau, T) d\tau}{1 - i\omega\tau} \quad (3)$$

where $\epsilon(0, T)$ is the low-frequency dielectric constant. As shown by Courtens (1984, 1986), for a broad relaxation time distribution function $g(\tau, T)$ in $\ln \tau$, $\epsilon''(\omega, T)$ can be approximated as

$$\epsilon''(\omega, T) \simeq \frac{\pi}{2} \epsilon(0, T) g\left(\frac{1}{\omega}, T\right). \quad (4)$$

Thus, the spectrum of dielectric loss gives direct information about $g(1/\omega, T)$. In the limit of $\tau_{\min} \leq 1/\omega \leq \tau_{\max}$, one can also obtain an important simple relation between real and imaginary parts of the dielectric permittivity (Ginzburg 1989, Lindgren *et al* 1981, Colla *et al* 1992):

$$\epsilon''(\omega, T) \simeq \frac{\pi}{2} \frac{\partial \epsilon'(\omega, T)}{\partial (\ln \omega)}. \quad (5)$$

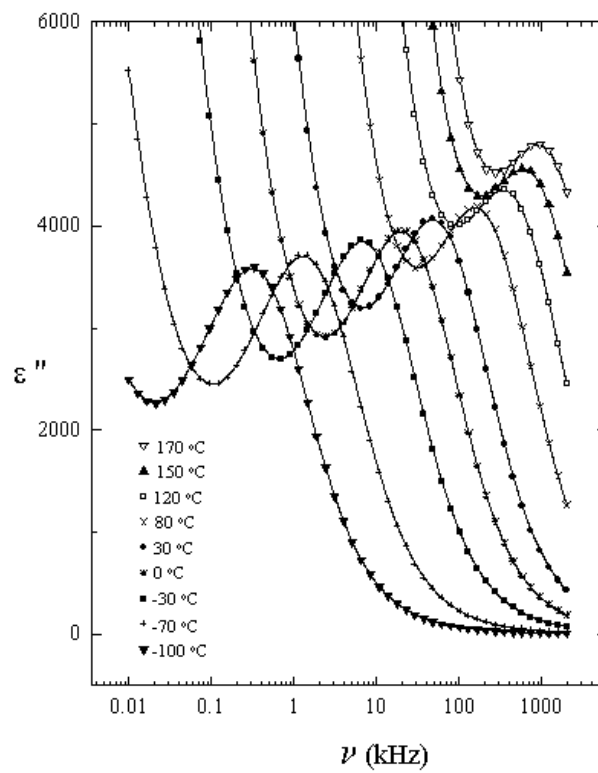


Figure 6. The frequency dependence of ϵ'' for BFN at various temperatures.

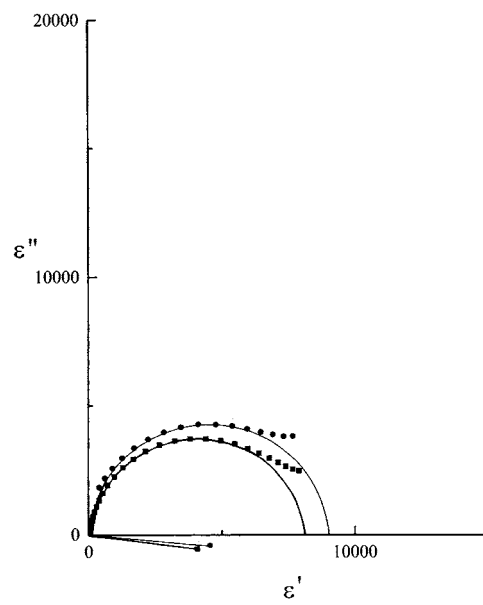


Figure 7. Cole-Cole plots at temperatures of -70 (squares) and 100 °C (circles) for BFN.

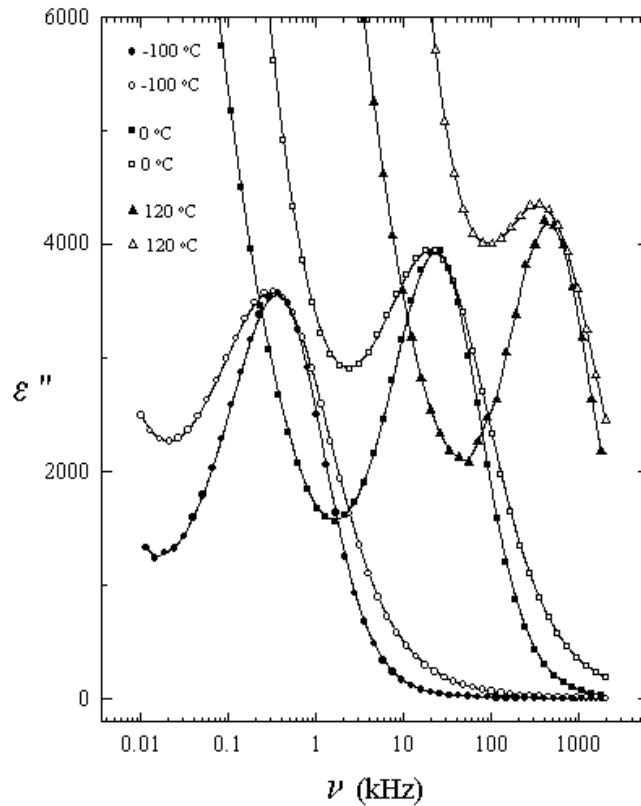


Figure 8. Comparison of the measured imaginary part of the dielectric permittivity of BFN with that calculated from equation (5) for three different temperatures, where the solid and open symbols represent the calculated and experimental points respectively.

We have used our experimental data to verify the validity of the assumptions made to get equation (5). The results obtained are shown in figure 8. The good agreement between the directly measured value of ϵ'' and those calculated from the dispersion of ϵ' using equation (5) suggests that the spectrum $g(1/\omega, T)$ is broad at low temperature as well as at high temperature.

Now returning to (4), if the frequency-independent term $(\pi/2)\epsilon(0, T)$ on the right-hand side is ignored, $\epsilon''(\omega, T)$ directly corresponds to the relaxation time distribution function $g(1/\omega, T)$. If we plot the $\epsilon''(\omega, T)$ data in scaled coordinates, i.e., $\epsilon''(\omega, T)/\epsilon''(\omega_m, T)$ and $\log(\omega/\omega_m)$, where ω_m corresponds to the frequency of the loss peak in the ϵ'' versus $\log \nu$ plots, the entire set of dielectric loss data can be collapsed onto one master curve as shown in figure 9. The scaling behaviour of $\epsilon''(\omega, T)$ clearly indicates that the distribution function for relaxation times is nearly temperature independent, and thus not much significance can be attached to the small variation in the Cole–Cole plot variable α with decreasing temperature. A similar collapse of the $\epsilon''(\omega, T)$ data onto one single curve has been demonstrated by Colla *et al* (1992) for PMN in the temperature range $-88 < T < -13$ °C.

Figure 10 shows the room temperature Mössbauer spectrum of the sample of BFN. The spectrum was fitted with a Lorentzian doublet giving an isomer shift = 0.43 mm s^{-1} and the quadrupole splitting = 0.54 mm s^{-1} , with iron being trivalent in octahedral coordination.

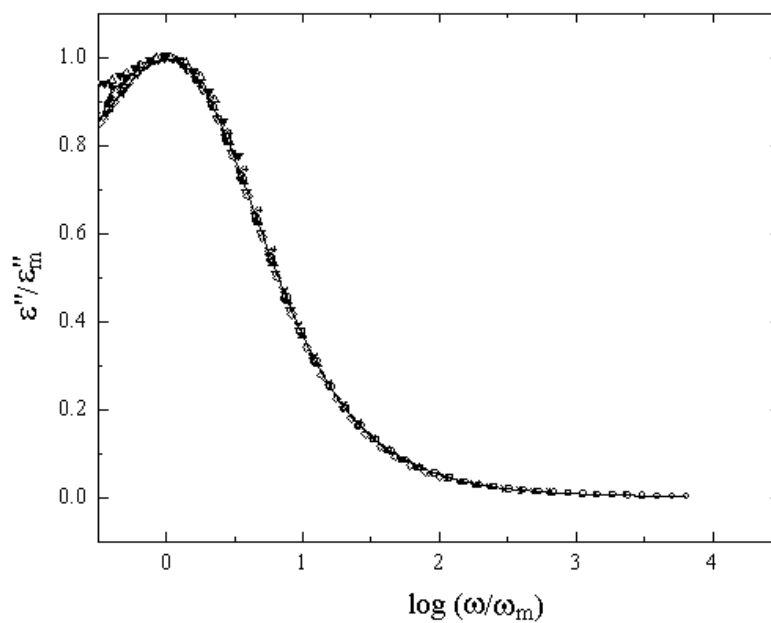


Figure 9. Scaling behaviour of ϵ'' at various temperatures for BFN.

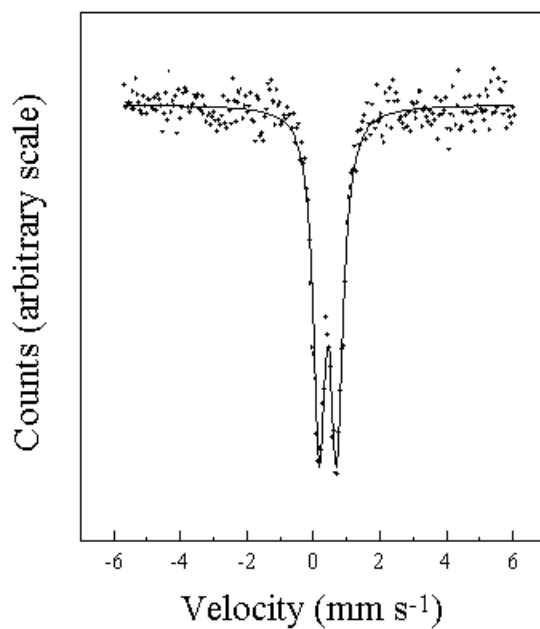


Figure 10. The Mössbauer spectrum of BFN at room temperature obtained using ^{57}Co diffused into rhodium as a source of gamma rays.

All attempts to use two doublets with the aim of checking for the eventual presence of any other iron (III) site gave unreliable results. The substantial quadrupole splitting observed in the paramagnetic spectrum confirms that the local symmetry at iron (III) sites is not cubic.

4. Conclusions

Ferroelectric BFN ceramic is synthesized by the solid-state reaction technique for the first time. The x-ray diffraction of the sample at room temperature shows a monoclinic phase. Dielectric studies of the sample performed at low frequencies show that T'_m and T''_m become frequency dependent. The temperature variations in ϵ' and ϵ'' become diffuse with T''_m being lower than T'_m . There is evidence for Vogel–Fulcher-type relaxational freezing below T'_m . The analysis of the ϵ' and ϵ'' versus $\log \nu$ data has been performed assuming a distribution of relaxation times as confirmed by Cole–Cole plots as well as the scaling behaviour of the dielectric loss. All these observations clearly suggest that BFN is a relaxor ferroelectric. The Mössbauer spectrum of the sample at room temperature shows a symmetric doublet, with the iron being trivalent. The quadrupole splitting observed in the paramagnetic spectrum shows that the local symmetry at iron (III) sites is not cubic.

References

- Beleckas B, Grigas J and Stefanovich S 1989 *Litov. Fiz. Sb.* **29** 202
- Bhat K C, Keer H V and Biswa A B 1974 *J. Phys. D: Appl. Phys.* **7** 2077
- Bokov A A, Mylnikova I E and Smolensky G A 1962 *Sov. Phys.–JETP* **42** 643
- Bokov V A, Shpak L A and Rayevsky I P 1993 *J. Phys. Chem. Solids* **54** 495
- Bonny V, Bonin M, Sciau P, Schenk K J and Chapuis G 1997 *Solid State Commun.* **102** 347
- Brunskill I H, Schmid H and Tissot P 1981 *Ferroelectrics* **37** 547
- Christen H M, Sommer R, Yushin N K and van der Klink J J 1994 *J. Phys.: Condens. Matter* **6** 2631
- Cole K S and Cole R H 1941 *J. Chem. Phys.* **9** 341
- Colla E V, Koroleva E Y, Okuneva N M and Vakhrushev S B 1992 *J. Phys.: Condens. Matter* **4** 3671
- Courtens E 1984 *Phys. Rev. Lett.* **52** 69
- Courtens E 1986 *Phys. Rev. B* **33** 2975
- Darlington C N W 1991 *J. Phys.: Condens. Matter* **3** 4173
- Elissalde C, Ravez J and Gaucher P 1992 *Mater. Sci. Eng. B* **13** 327
- Fulcher G S 1925 *J. Am. Ceram. Soc.* **8** 339
- Ginzburg S L 1989 *Irreversible Phenomena of Spin Glasses* (Moscow: Nauka)
- Hochli U T, Knorr K and Loidl A 1990 *Adv. Phys.* **39** 405
- Ivanov S A, Tellgren R, Rundlof H, Thomas N W and Ananta S 2000 *J. Phys.: Condens. Matter* **12** 2393
- Lampis N, Sciau P and Lehmann A G 1999 *J. Phys.: Condens. Matter* **11** 3489
- Lemanov V V, Yushin N K, Smirnova E P, Potnikov A P, Tarakanov E A and Maksimov A Y 1992 *Ferroelectrics* **134** 139
- Lindgren L, Svedlindh P and Beckman O 1981 *J. Magn. Magn. Mater.* **25** 33
- Mabud S A 1984 *Phase Transitions* **4** 183
- Rayevsky I P, Bokov A A, Bogatin A S, Emelyanov S M, Malitskaya M A and Prokopalo O I 1992 *Ferroelectrics* **126** 191
- Schmid H 1994 *Ferroelectrics* **162** 317
- Smolensky G A 1970 *J. Phys. Soc. Japan* **28** 26
- Smolensky G A 1984 *Ferroelectrics* **53** 129
- Smolensky G A, Agranovskaya A I, Popov S N and Isupov V A 1958 *Sov. Phys.–Tech. Phys.* **3** 1981
- Vakhrushev S, Zhukov S, Fetisov G and Chernyshov V 1994 *J. Phys.: Condens. Matter* **6** 4021
- Viehland D, Jang S J, Cross L E and Wuttig M 1990 *J. Appl. Phys.* **68** 2916
- Viehland D, Jang S J, Cross L E and Wuttig M 1991 *Phil. Mag. B* **64** 335
- Vogel H 1921 *Z. Phys.* **22** 645
- Wagner K W 1913 *Ann. Phys., Lpz.* **40** 817
- Yasuda N and Ueda Y 1989a *J. Phys.: Condens. Matter* **1** 497
- Yasuda N and Ueda Y 1989b *J. Phys.: Condens. Matter* **1** 5179
- Yokosuka M 1993 *Japan. J. Appl. Phys.* **32** 1142
- Yushin N K and Dorogovtsev S N 1993 *Ferroelectrics* **143** 49